Preparation and characterisation of high refractive index $PbO–TiO_2–TeO_2$ glass systems

Raul F. Cuevas,[a] Ana M. de Paula,[a] Oswaldo L. Alves,[b] Norberto Aranha,[a] José A. Sanjurjo,[a] Carlos L. Cesar[a] and Luiz C. Barbosa*[,a]

[a]*Instituto de Física, Universidade Estadual de Campinas, Caixa Postal 6165, 13083-970 Campinas-SP, Brazil*
[b]*Instituto de Química, Universidade Estadual de Campinas, Caixa Postal 6154, 13083-970 Campinas-SP, Brazil*

We describe the preparation and characterisation of high refractive index $PbO–TiO_2–TeO_2$ glass systems. Highly homogeneous glasses were obtained by agitating the oxide mixture during the melting process in an alumina crucible. The characterisation was performed by X-ray diffraction, density, dilatometry, Raman scattering, light absorption and linear refractive index measurements. The results show a change in the glass structure as the PbO content increases: the TeO_4 trigonal bipyramids characteristic of TeO_2 glasses transform into TeO_3 trigonal pyramids. However, the measured refractive indices are almost independent of the glass composition. We show that third-order non-linear optical susceptibilities calculated from the measured refractive indices using Lines' theoretical model are also independent of the glass composition.

Tellurium oxide-based glasses are potential materials for optical device applications due to their non-linear optical properties. They show high refractive indices, and consequently high third-order non-linear susceptibilities $\chi^{(3)}$, and high relative permittivities.[1,2] Also, they are transparent over the visible and near IR regions. Kim *et al.*[3] have measured for a pure TeO_2 glass a value of $\chi^{(3)} = 1.41 \times 10^{-12}$ esu; however, it is not easy to obtain this pure glass. Some recent works have shown that the addition of TiO_2, PbO and Nb_2O_5 increases the glass stability and refractive index.[4–7] In particular, the $PbO–TiO_2–TeO_2$ glass systems have presented the highest $\chi^{(3)}$ values, in the range 2×10^{-12} to 4×10^{-12} esu.[5,6] Nonetheless, the dependence of the non-linear properties on the concentration of the three components is not yet clearly established. The discrepancies in the measured $\chi^{(3)}$ values are still quite high, probably due to inhomogeneities in the glasses.[5,6]

In this work we present a study of the properties of this glass system as a function of the PbO composition. We have synthesised $x\text{PbO}:10\text{TiO}_2:(100-x)\text{TeO}_2$ glasses with $x = 5$, 10, 15, 20 and 25 mol%. We obtained highly homogeneous glasses by agitating the mixture during the melting process. The glasses were characterised by means of X-ray diffraction (XRD), density, dilatometry, Raman scattering, optical absorption and linear refractive index measurements. Most of the measured properties show the previously observed[6,8] change in the glass structure as the PbO content increases: the TeO_4 trigonal bipyramids characteristic of TeO_2 glasses break into TeO_3 trigonal pyramids. Nonetheless, the measured refractive indices are almost independent of the glass composition. Calculated $\chi^{(3)}$ values using Lines' theoretical model[9,10] are also independent of the glass composition.

Experimental

We studied a series of five $x\text{PbO}:10\text{TiO}_2:(100-x)\text{TeO}_2$ glass samples with $x = 5$, 10, 15, 20 and 25 mol%, which we denote as PTT1, PTT2, PTT3, PTT4, and PTT5, respectively (see Table 1). The materials used were reagent-grade TiO_2 (Merck), TeO_2 (Merck) and PbO (Riedel). A batch of 25 g of the mixture for each composition was placed directly in an alumina crucible in an electric furnace. The mixture was agitated during the melting process in order to obtain homogeneous concentrations. Melting was achieved at 900 °C for 20 min. The melt was quenched between a pair of stainless-steel plates and later annealed for 2 h at 300 °C. The samples were prepared in two forms: powder for the XRD, and approximately 1 mm thick slabs for the other measurements.

The glassy state was confirmed by X-ray diffraction analysis using Cu-Kα radiation in a Shimadzu difractometer. The densities were determined by the pycnometer method using helium as the displacement gas. The thermal properties were measured with a Harrop conventional horizontal dilatometer. The Raman spectra were measured using the argon ion laser line at 514.5 nm at backscattering geometry and a triple Jobin-Yvon spectrometer with multichannel detection. The absorption measurements were obtained using a Perkin-Elmer Lambda 9 spectrophotometer.

For the refractive index measurements we used a manual Rudolph null ellipsometer (model 436) with a 150 W tungsten lamp as a light source. The desired wavelengths were selected by interference filters. The output power of the ellipsometer optics was measured with a commercial liquid-nitrogen-cooled InAs detector, whose signal was integrated by a lock-in amplifier. The use of a less noisy detector instead of the cooled PbS detector supplied by the manufacturer proved to be essential to achieve experimental errors as low as 0.1%.

Results and Discussion

Glass formation

The preparation procedure described in the Experimental section permitted us to obtain bubble-free transparent glasses with high homogeneity and a yellowish colour. All the compositions showed the XRD patterns typical for a glass phase presenting a halo near $2\theta = 22.5°$.

Density

Fig. 1 shows the glass density dependence on the PbO concentration. The density increases almost linearly with increasing PbO content. This is an indication that the PbO enters the glass structure as a network modifier. The linear behaviour may be explained by the fact that TeO_2 was substituted by the heavier PbO.

Dilatometry

The glass-transition temperatures (T_g), the softening-point temperatures (T_d) and the thermal expansion coefficients (κ) are

Table 1 Parameters used in the $\chi^{(3)}$ calculations and the obtained values considering $f=1.72$

glass	composition (mol%)	n at 1.907 μm	f_L	E_0/eV	I_d/Å	$\chi^{(3)}/10^{-12}$ esu
PTT1	$5PbO:10TiO_2:85TeO_2$	1.871	1.834	4.87	1.923	3.49
PTT2	$10PbO:10TiO_2:80TeO_2$	1.850	1.808	4.73	1.932	3.48
PTT3	$15PbO:10TiO_2:75TeO_2$	1.854	1.813	4.75	1.942	3.54
PTT4	$20PbO:10TiO_2:70TeO_2$	1.855	1.814	4.78	1.952	3.54
PTT5	$25PbO:10TiO_2:65TeO_2$	1.854	1.813	4.73	1.962	3.63

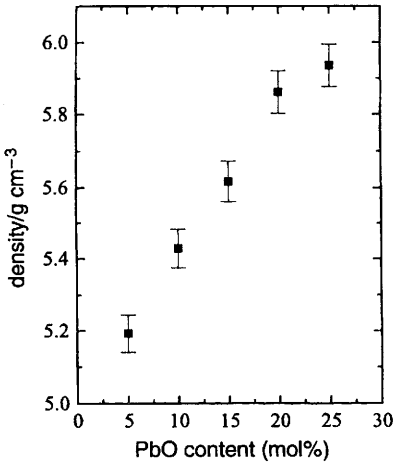

Fig. 1 The PTT glass density dependence on the glass composition

shown in Fig. 2 as a function of the PbO content. The temperatures T_g and T_d decrease linearly with increasing PbO concentration, whereas the thermal expansion coefficient shows a linear increase with the PbO content. A decrease in T_g and T_d usually indicates a more open glass network, whereas a increase in the thermal expansion coefficient indicates weaker bonds, as weaker bonds increases the anharmonic contributions of the inter-ionic potentials to the thermal expansion. When the PbO enters the glass structure as a network modifier, some of the Te—O bonds are broken with TeO_4 trigonal bipyramids transforming into TeO_3 trigonal pyramids with non-bridging oxygen.[6,8] This transformation weakens the Te—O bonds and opens the glass network, and may explain the observed dependence on PbO concentration.

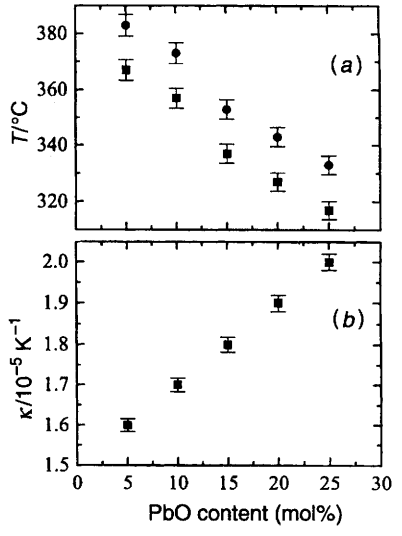

Fig. 2 Thermal properties of the PTT glass system as a function of the PbO content. The transition (T_g; ■) and softening (T_d; ●) glass temperatures are shown in (*a*) and the thermal expansion coefficient (κ) in (*b*).

Raman spectra

The Raman spectra from the PTT glasses are presented in Fig. 3. We observed the following features in the spectra: a band at 135 cm^{-1} which is assigned to the PbO vibrations,[8] a broad band at *ca.* 478 cm^{-1} which is assigned to Te—O—Te bending modes,[11] whose intensity decreases as the PbO content increases. The two bands observed at *ca.* 682 and 773 cm^{-1} have been assigned to the stretching vibrations of TeO_4 trigonal bipyramids, characteristics of TeO_2 glasses, and stretching vibrations of the TeO_3 trigonal pyramids, respectively.[8,11] Note that as the PbO content increases the intensity of the TeO_3 band increases relative to that of the TeO_4 band, and the TeO_3 band is the most intense band for the samples PTT4 and PTT5. Also these bands shift slightly to lower Raman energy as the PbO concentration increases. There is also a weak band at *ca.* 300 cm^{-1} for PbO contents greater than 15 mol%, which has been assigned to the bending vibrations of TeO_3 trigonal pyramids with non-bridging oxygen. These results are consistent with the structural change observed for $PbO–TeO_2$ glass systems; as the PbO content increases the TeO_4 trigonal bipyramids break into TeO_3 trigonal pyramids. Nonetheless, this change is slower when compared to $Li_2O–TiO_2–TeO_2$ glasses.[7] Yamamoto *et al.*[5] presented quantitative measurements of the Te coordination number in these two glass systems that showed this same trend.

Optical absorption

We have measured the glass transmission in the wavelength range 300–1500 nm. The transmittance data are shown in the inset of Fig. 4 for samples PTT1 and PTT2, the curves are almost flat from 800 to 1500 nm. The curves for the other samples (PTT3 to PTT5) are indistinguishable from the PTT2 curve. The UV–VIS cut-off wavelength is at *ca.* 420 nm for all compositions.

From the transmission curve we calculated the optical absorption coefficient, α. In order to obtain the optical energy gap we plotted $(\alpha E)^2$ as a function of energy E. Fig. 4 shows the curves for samples PTT1 and PTT2. The values of the optical energy gap were obtained from the extrapolation of the linear regions of the plots to $(\alpha E)^2=0$. The optical gap is at *ca.* 2.94 eV for all the PbO compositions.

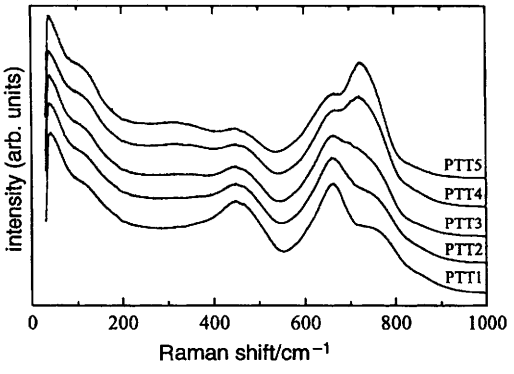

Fig. 3 Raman spectra of the PTT glass system. The spectra have been arbitrarily shifted vertically for clarity.

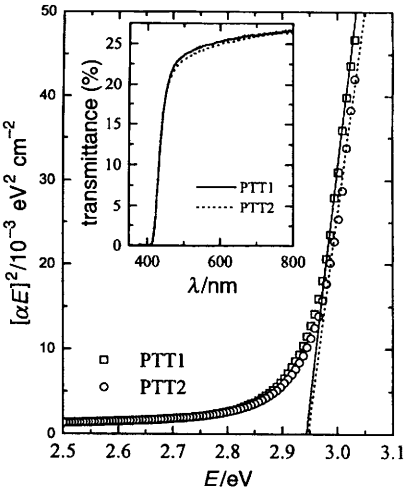

Fig. 4 Plot of $(\alpha E)^2$ as a function of energy for the PTT glass system, the curves for the PTT3, PTT4 and PTT5 glasses are indistinguishable from the curve for the PTT2 glass. The solid and dashed lines are the linear fits to obtain the optical gap for PTT1 and PTT2 samples, respectively. The inset shows the transmission curves.

Linear refractive index

We have measured the linear refractive index, n, of the glasses for wavelengths centred at 546, 633, 800, 1300, 1750 and 2000 nm. The bandwidth of the used filters was 70 nm. The results are listed in Table 2, the experimental errors are *ca.* 0.1%. Fig. 5 shows the linear refractive index dispersion, the solid lines are extrapolation curves. In Fig. 6 the refractive index is plotted as a function of PbO content for all the measured wavelengths. Note that there is just a small change with the PbO content: the values for the PTT1 sample are slightly larger than for the other samples at the high wavelength region. Also plotted in Fig. 6 are the linear refractive index data at 632.8 nm (crosses) from Yamamoto *et al.*[6] The values are comparable; however, their results show an increasing trend with PbO content, which we do not observe.

Table 2 Measured refractive indices as function of wavelength for the PTT glasses

	refractive index, n				
wavelength/nm	PTT1	PTT2	PTT3	PTT4	PTT5
546	2.204	2.209	2.208	2.207	2.208
633	2.150	2.152	2.153	2.151	2.152
800	2.088	2.085	2.085	2.086	2.084
1300	1.990	1.981	1.983	1.981	1.983
1750	1.907	1.891	1.892	1.893	1.892
2000	1.852	1.835	1.835	1.836	1.834

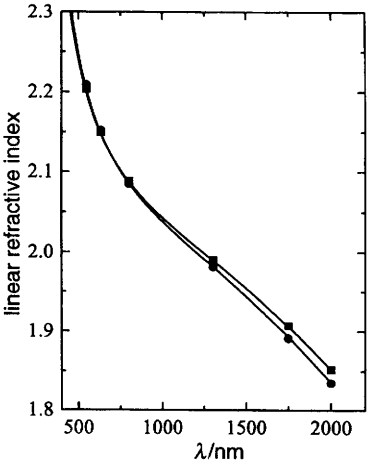

Fig. 5 Linear refractive index as a function of wavelength for the PTT glass system: ■, PTT1; ●, PTT2. The results for the PTT3, PTT4 and PTT5 are indistinguishable from those for the PTT2 glass. The lines are extrapolation curves.

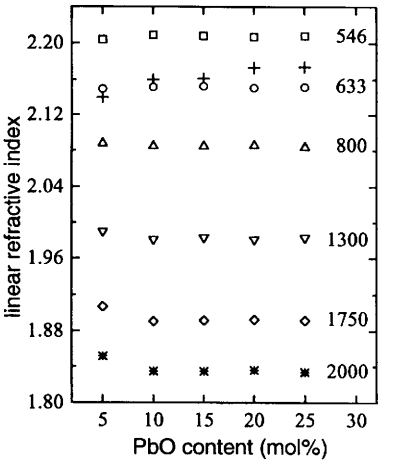

Fig. 6 Linear refractive index of the PTT glass system as a function of the PbO content. The wavelengths in nm are indicated at the right side of the plot. The crosses are the data of Yamamoto *et al.*[6]

We have calculated E_d and E_o using the expression for n as a function of the energy E proposed by Wemple:[12] $1/(n^2-1) = E_o/E_d - E^2/(E_o E_d)$, where E_o is the average excitation energy for electronic transition and E_d is the electronic oscillator strength related to dispersion. The E_o values (listed in Table 1) are used to calculate the non-linear refractive index.

Non-linear refractive index

To calculate the non-linear refractive index we used Lines' bond-orbital theory,[9,10] which considers the influence of cationic empty d-orbital on the glass non-linear optical response. The contribution of the d-orbital to the non-linear response is proportional to the decrease of the bond length between cation and anion, l_d, and to the increase of the orbitals overlap $\langle d|p \rangle$. He studied a number of transparent transition-metal oxides and found that this contribution is negligible for bond lengths $l_d > 2.3$ Å, but increases rapidly as the bond length decreases and becomes dominant for $l_d < 2.0$ Å. The non-linear optical response was obtained using a variational method to describe the effect of an applied electric field $f\boldsymbol{E}_x$ along the bond direction x in the perturbed molecular orbital. The factor f takes into account any local field enhancement or shielding effects. The frequency-dependent non-linear refractive index, n_2, is expressed by the empirical formula:[10]

$$n_2(\text{av.})/10^{-13}\ \text{esu} = \frac{25 f^3 f_L^3 l_d^2 (n^2-1) E_s^6}{n(E_s^2 - \hbar^2\omega^2)^4} \qquad (1)$$

where $f_L = (n^2+2)/3$ is the Lorentzian local-field enhancement factor,[9] n is the long-wavelength limit value of the refractive index, E_s in eV is the effective Sellmeier energy gap which takes in account the contributions of the sp and d orbitals, and l_d in Å is the bond length for the ternary glass. The Sellmeier gap is in practice equal to E_o in Wemple's equation;[12] values are listed in Table 1. The bond lengths for the ternary glasses were estimated using the method proposed by Nassau,[13] with the Pb—O, Ti—O and Te—O bond lengths as 2.24, 1.96 and 1.91 Å, respectively.[10] Also, we used the following equation[9] to convert n_2 into $\chi^{(3)}$:

$$\chi^{(3)}(-3\omega,\omega,\omega,\omega)/\text{esu} = \frac{n}{3\pi} n_2(\text{av.}) \qquad (2)$$

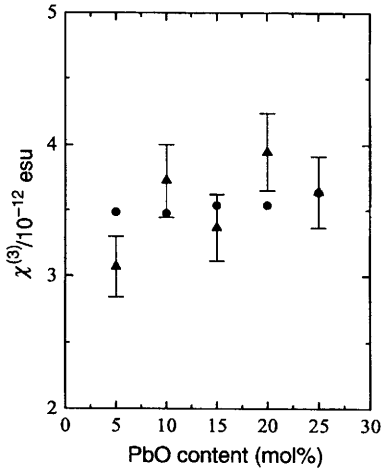

Fig. 7 Third-order susceptibility $\chi^{(3)}$ as a function of the PbO content for the PTT glass system. The triangles represent the data from Yamamoto *et al.*[6] and the circles are our calculated values.

The estimated $\chi^{(3)}$ at the wavelength of 1.907 μm (the wavelength for the measured data of Yamamoto *et al.*[6]) are given in Table 1 and plotted in Fig. 7 (circles), for the PTT glasses. Note that the results are almost independent of the PbO content. To compare our results with the data of Yamamoto *et al.*[6] (triangles) we have used $f=1.72$, we chose to make the values of $\chi^{(3)}$ equal to the experimental value for the PbO content of 25 mol%. This f value is close to the value of 1.9 ± 0.1 obtained by Lines[10] for transition-metal oxides dominated by d-band responses. This is an indication that Lines' model, which assumes that the high non-linear optical response is due to virtual excitations from the cationic sp levels to virtual d levels, is valid for TeO_2-based glasses. Kim *et al.*[3] have already shown that this model can be used for a TeO_2 pure glass, where the most probable optical transition is the electron transfer from $2p_\pi$ orbitals of the oxygen to the empty non-bonding 5d orbitals of tellurium. We have also shown that this model holds for the Li_2O–TiO_2–TeO_2 glass system.[7]

It should be pointed out that for the Li_2O–TiO_2–TeO_2 glass system the refractive index and $\chi^{(3)}$ decrease as the TeO_2 is substituted by the Li_2O, owing to the change of TeO_4 trigonal bibyramids into TeO_3 trigonal pyramids. One would then expect that slower structure changes in the PbO–TiO_2–TeO_2 glasses would result in a slow decrease in the refractive index. Nonetheless, the measured values are almost independent of the PbO content. Thus, the presence of the PbO should increase the refractive index to compensate for the decrease due to the glass structure change.

Conclusions

We present highly homogeneous PbO–TiO_2–TeO_2 glasses with high refractive indices. The density, softening-point temperature, glass-transition temperature, thermal expansion coefficient and Raman peaks were found to depend on the PbO content. In contrast, the UV–VIS cut-off, optical gap and the linear refractive index were found to be almost independent of the PbO content. These trends are consistent with a glass structure change, with TeO_4 trigonal bipyramids breaking into TeO_3 trigonal pyramids as the PbO content increases. The almost constant refractive indices may be explained by two opposing contributions. The PbO itself increases the refractive index; however, the increase in PbO content also increases the breaking of TeO_4 trigonal bipyramids into TeO_3 trigonal pyramids, which decreases the refractive index. Nonetheless, the $\chi^{(3)}$ values are larger than those of the pure TeO_2 glasses.

The authors acknowledge the Conselho Nacional de Desenvolvimento Cientifico e Tecnológico (CNPq), Fundação de Amparo à Pesquisa do Estado de São Paulo (FAPESP), Programa de Apoio ao Desenvolvimento Científico e Tecnológico (PADCT) and the Telecomunicações Brasileiras S/A (Telebras) for financial support.

References

1 S. Inoue and A. Nukui, in *Proc. Int. Conf. on Science and Technology of New Glasses*, ed. S. Sakka and N. Soga, The Ceramic Society of Japan, Tokyo, 1991, p. 77.
2 H. Nasu, Y. Ibara and K. Kubodera, *J. Non-Cryst. Solids*, 1989, **110**, 229.
3 S-H. Kim, T. Yoko and S. Sakka, *J. Am. Ceram. Soc.*, 1993, **76**, 2486.
4 H. Nasu, O. Matsushita, H. Kamiya, H. Kobayashi and K. Kubodera, *J. Non-Cryst. Solids*, 1990, **124**, 275.
5 H. Nasu, O. Matsushita, H. Kamiya, H. Kobayashi and K. Kubodera, *Jpn. J. Appl. Phys.*, 1992, **31**, 3899.
6 H. Yamamoto, H. Nasu, J. Matsuoka and K. Kamiya, *J. Non-Cryst. Solids*, 1994, **170**, 87.
7 R. F. Cuevas, L. C. Barbosa, A. M. de Paula, Y. Liu, V. C. S. Reynoso, O. L. Alves, N. Aranha and C. L. Cesar, *J. Non-Cryst. Solids*, 1995, **191**, 107.
8 S. Khatir, F. Romain, J. Portier, S. Rossignol, B. Tanguy, J. J. Videau and S. J. Turrel, *J. Mol. Struct.*, 1993, **298**, 13.
9 M. E. Lines, *Phys. Rev. B*, 1990, **41**, 3372; 3383.
10 M. E. Lines, *Phys. Rev. B*, 1991, **43**, 11978.
11 T. Sekiya, N. Mochida, A. Ohtsuka and M. Tonokawa, *J. Non-Cryst. Solids*, 1992, **144**, 128.
12 S. H. Wemple, *J. Chem. Phys.*, 1977, **67**, 2151.
13 K. Nassau, *Electron Lett.*, 1981, **17**, 769; *Bell. Syst. Tech. J.*, 1981, **60**, 327.

Paper 6/02829B; *Received* 23*rd April*, 1996